

Making Human-Like Trade-offs in Constrained Environments by Learning from Demonstrations

Arie Glazier¹ Andrea Loreggia² Nicholas Mattei¹
 Taher Rahgooy³ Francesca Rossi³ K. Brent Venable^{3,5}

¹ Tulane University, New Orleans, LA, USA

² European University Institute, Italy

³ University of West Florida, Pensacola, FL, USA

⁴ IBM Research, Yorktown Heights, NY, USA

⁵ Institute for Human and Machine Cognition, Pensacola, FL, USA

adglazier@gmail.com, andrea.loreggia@gmail.com, nsmattei@tulane.edu
 trahgooy@students.uwf.edu, Francesca.Rossi2@ibm.com, bvenable@ihmc.org

Abstract

Many real-life scenarios require humans to make difficult trade-offs: do we always follow all the traffic rules or do we violate the speed limit in an emergency? These scenarios force us to evaluate the trade-off between collective norms and our own personal objectives. To create effective AI-human teams, we must equip AI agents with a model of how humans make trade-offs in complex, constrained environments. These agents will be able to mirror human behavior or to draw human attention to situations where decision making could be improved. To this end, we propose a novel inverse reinforcement learning (IRL) method for learning implicit hard and soft constraints from demonstrations, enabling agents to quickly adapt to new settings. In addition, learning soft constraints over states, actions, and state features allows agents to transfer this knowledge to new domains that share similar aspects. We then use the constraint learning method to implement a novel system architecture that leverages a cognitive model of human decision making, multi-alternative decision field theory (MDFT), to orchestrate competing objectives. We evaluate the resulting agent on trajectory length, number of violated constraints, and total reward, demonstrating that our agent architecture is both general and achieves strong performance. Thus we are able to capture and replicate human-like trade-offs from demonstrations in environments when constraints are not explicit.

1 Introduction

Implicit and explicit constraints are present in many decision making scenarios, and they force us to make difficult decisions: do we always satisfy all constraints, or do we violate some of them in exceptional circumstances? Many techniques can be used to combine constraints and goals so that the agent rationally minimizes constraint violations while achieving the given goal (Noothigattu et al. 2019). However, it is well known that humans are not rational. When we need to make a decision in a constrained environment, we often reason by employing heuristics and approximations which are subject to bias and noise (Busemeyer and Diederich 2002; Booch et al. 2021). This means that opti-

mal techniques may not be suitable if the aim is to design autonomous artificial agents that act like humans, or decision support systems that simulate human behavior to anticipate it and possibly alert humans by making them aware of their reasoning and inference deficiencies.

Moreover, these constraints are often not explicitly given, but need to be inferred from observations of how other agents act in the constrained world. Learning constraints from demonstrations is an important topic in the domains of inverse reinforcement learning (Scobee and Sastry 2020; Abbeel and Ng 2004), which is used to implement AI safety goals including value alignment (Russell, Dewey, and Tegmark 2015) and to circumvent reward hacking (Amodei et al. 2016; Ray, Achiam, and Amodei 2019). Recent work has focused on building ethically bounded agents (Svegliato, Nashed, and Zilberstein 2021; Rossi and Mattei 2019) that comply with ethical or moral theories of action. Following the work of Scobee and Sastry (2020), we propose an architecture that, given access to a model of the environment and to demonstrations of constrained behavior, is able to learn constraints associated with states, actions, or state features. Our method, MESC-IRL, performs comparably with the state of the art and is more general, as it can handle both hard and soft constraints in both deterministic and non-deterministic environments. It is also decomposable into features of the environment, supporting the transfer of learned constraints between environments.

Once the constraints are learned, we turn our attention to *making human like trade-offs*. Enabling agents to make trade-offs like humans allows them to mirror human behavior or to draw human attention to situations where decision making could be improved (Booch et al. 2021). Additionally, making these trade-offs explicit enables decision support tools that are able to mirror the goals of human decision makers (Balakrishnan et al. 2018, 2019). We propose a novel orchestration technique leveraging Multi-Alternative Decision Field Theory (MDFT) (Busemeyer and Diederich 2002), a decision making framework which is based on a psychological theory of how humans make decisions that is

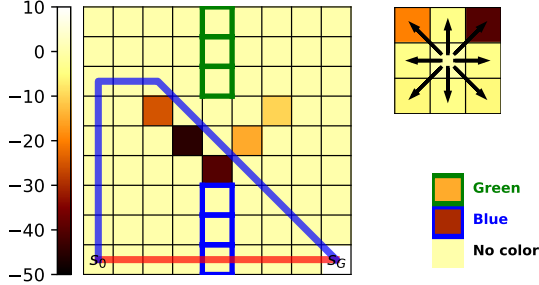


Figure 1: Grid with constraints of varying costs over actions (top right), state occupancy (grid, left) and state features (bottom right). Note that $\pi_{\mathcal{N}}^*$ for $\mathcal{M}^{\mathcal{N}}$ is the red trajectory, obtained by an agent that does not know the constraints while $\pi_{\mathcal{C}^*}^*$ for $\mathcal{M}^{\mathcal{C}^*}$ is the blue trajectory.

able to capture deviations from rationality observed in humans, making trade-offs between competing objectives in a more human-like way. We compare this MDFT-based orchestrator with other methods both theoretically and empirically, showing that our architecture is theoretically more expressive and obtains better empirical performance across a range of metrics when acting in constrained environments. The goal here is to use a cognitive model to capture the sometimes irrational decisions made by humans. Building machines that *act* more like humans is a step to create effective human-machine teams or decision support systems.

2 Preliminaries and Related Work

We begin this section by providing the preliminary notions on the context of our work, that is, constrained Markov Decision Processes and Reinforcement Learning (Sutton and Barto 2018). We then review fundamental concepts and methods on Inverse Reinforcement Learning (Ng and Russell 2000; Abbeel and Ng 2004) and background on Constrained Markov Decision Processes (Altman 1999) including related work on learning constraints (Ziebart et al. 2008; Malik et al. 2021; Scobee and Sastry 2020), which we will leverage to develop our novel method for learning soft constraints (Rossi, Van Beek, and Walsh 2006) from demonstrations (Chou, Berenson, and Ozay 2018). We conclude this section presenting a short review of the Multi-Alternative Decision Field Theory (Busemeyer and Diederich 2002), the cognitive model of decision making which will be at the core of our novel approach to orchestrating competing objectives.

2.1 Markov Decision Processes and Reinforcement Learning

A finite-horizon Markov Decision Process (MDP) \mathcal{M} is a model for sequential decision making over a number of time steps $t \in T$ defined by a tuple $(\mathcal{S}, \mathcal{A}, P, D_0, \phi, \gamma, R)$ (Sutton and Barto 2018). \mathcal{S} is a finite set of discrete states; $\{\mathcal{A}_s\} \subseteq \mathcal{A}$ is a set of actions available at state s ; $P : \mathcal{S} \times \mathcal{A} \times \mathcal{S} \rightarrow [0, 1]$ is a model of the environment given

as transition probabilities where $P(s_{t+1}|s_t, a_t)$ is the probability of transitioning to state s_{t+1} from state s_t after taking action $a_t \in \{\mathcal{A}_{s_t}\}$ at time t . $D_0 : \mathcal{S} \rightarrow [0, 1]$ is a distribution over start states; $\phi : \mathcal{S} \times \mathcal{A} \times \mathcal{S} \rightarrow \mathbb{R}^k$ is a mapping from the transitions to a k -dimensional space of features; $\gamma \in [0, 1]$ is a discount factor; and $R : \mathcal{S} \times \mathcal{A} \times \mathcal{S} \rightarrow \mathbb{R}$ is a scalar reward received by the agent for being in one state and transitioning to another state at time t , written as $R(s_t, a_t, s_{t+1})$.

An agent acts within the environment defined by the MDP, generating a sequence of actions called a *trajectory* of length t . Let $\tau = ((s_1, a_1, s_2), \dots, (s_{t-1}, a_{t-1}, s_t)) \in (\mathcal{S} \times \mathcal{A} \times \mathcal{S})^t$. We evaluate the quality of a particular trajectory in terms of the amount of reward accrued over the trajectory, subject to discounting. Formally, $R(\tau) = \sum_{i=1}^t \gamma^i R(s_i, a_i, s_{i+1})$. A policy, $\pi : \mathcal{S} \rightarrow \mathcal{P}(\mathcal{A})$ is a map of probability distribution to actions for every state such that $\pi(s, a)$ is the probability of taking action a in state s . We can also write the probability of a trajectory τ under a policy as $\pi(\tau)$. The feature vector associated with trajectory τ is defined as the summation over all transition feature vectors in τ , $\phi(\tau) = \sum_{(s_t, a_t, s_{t+1}) \in \tau} \phi(s_t, a_t, s_{t+1})$.

The goal within an MDP is to find a policy π^* that maximizes the expected reward, $J(\pi) = \mathbb{E}_{\tau \sim \pi}[R(\tau)]$ (Malik et al. 2021). In the MDP literature, classical tabular methods are used to find π^* including value iteration (VI). Such method finds an optimal policy by estimating the expected reward for taking an action a in a given state s , i.e., the Q -value of pair (s, a) , written $q(s, a)$. (Sutton and Barto 2018).

2.2 Constrained MDPs and Inverse Reinforcement Learning

We are interested in learning constraints from demonstrations. Our goal is to create agents that are able to be trained to follow constraints that are not explicitly prohibited in the MDP, but should be avoided (Rossi and Mattei 2019). (Scobee and Sastry 2020) discusses the importance of such constraints: an MDP \mathcal{M} may encode everything necessary about driving a car, e.g. the dynamics of steering and movements, but often one wants to add additional general constraints such as *avoid obstacles on the way to the goal*. These constraints are often non-Markovian and engineering a reward function that encodes these constraints may be a difficulty or impossible task (Vazquez-Chanlatte et al. 2018).

One approach for learning constraints from demonstrations is to use techniques from inverse reinforcement learning (IRL): given a set of demonstrated trajectories \mathcal{D} of an agent in an environment \mathcal{M} with an unknown reward function $\mathcal{M} \setminus R$, IRL provides a set of techniques for learning a reward function \hat{R} that explains the agent’s demonstrated behavior (Abbeel and Ng 2004; Ng and Russell 2000). However, this technique has many drawbacks: often there are many reward functions that lead to the same behavior (Scobee and Sastry 2020), the reward functions may not be interpretable (Vazquez-Chanlatte et al. 2018), and there may be issues such as reward hacking – wherein the agent learns to behave in ways that create reward but are not intended by the designer – an important topic in the field of AI safety (Amodei et al. 2016; Ray, Achiam, and Amodei

2019) and value alignment (Rossi and Mattei 2019; Russell, Dewey, and Tegmark 2015).

We follow the framework of Altman (1999) and Malik et al. (2021) and define a Constrained MDP \mathcal{M}^C which is a nominal MDP \mathcal{M}^N with an additional cost function $\mathcal{C} : \mathcal{S} \times \mathcal{A} \times \mathcal{S} \rightarrow \mathbb{R}$ and a budget $\alpha \geq 0$. We can then define the cost of a trajectory to be $c(\tau) = \sum_{i=1}^t c(s_i, a_i, s_{i+1})$. Setting $\alpha = 0$ is enforcing *hard constraints*, i.e., we must never trigger constrained transitions. In this work, unlike the work of both Scobee and Sastry (2020) and Malik et al. (2021), we are interested in learning *soft constraints* (Rossi, Van Beek, and Walsh 2006). Under a soft constraints paradigm, each constraint comes with a real-valued penalty/cost and the goal is to minimize the sum of penalties incurred by the agent.

Following Scobee and Sastry (2020), the task of constraint inference in IRL is defined as follows. Given a nominal MDP \mathcal{M}^N and a set of demonstrations \mathcal{D} in ground-truth constrained world \mathcal{M}^{C^*} , we wish to find the most likely set of constraints \mathcal{C} that could modify \mathcal{M}^N to explain the demonstrations. We are concerned with three types of constraints:

Action Constraints. We may not want an agent to ever perform some (set of) action a_i .

Occupancy Constraints. We may not want an agent to occupy a (set of) states s_i .

Feature Constraints. Given a feature mapping of transitions ϕ , we may not want an agent to perform an (set of) action in presence of specific state features.

Without loss of generality, we add the state and actions to the features. Hence, action and occupancy become specific cases of feature constraints. Note that the set of constraints is defined as a cost function over the set of transitions $\mathcal{C} : \mathcal{S} \times \mathcal{A} \times \mathcal{S} \rightarrow \mathbb{R}$. In Scobee and Sastry (2020), this definition is limited to a set of state-actions $\mathcal{S} \times \mathcal{A}$ as they are assuming a deterministic setting and hence are able to define \mathcal{M}^C by substituting $\mathcal{A} = \{A_s\}$ with $\mathcal{A}^C = \{A_s^C\}$ in \mathcal{M}^N . Finally, both Scobee and Sastry (2020) and Malik et al. (2021) propose a greedy approach to infer a set of constraint \mathcal{C} that explains the demonstrations D on \mathcal{M}^{C^*} . In both Scobee and Sastry (2020) and Malik et al. (2021) the domain is restricted to deterministic MDPs, which we strictly generalize in this work; additionally Scobee and Sastry (2020), like our model, only works with discrete actions, while Malik et al. (2021) works for both discrete and continuous action sets. We also generalize to the non-deterministic setting; we additionally generalize to the setting of soft constraints, hence our task is to learn the cost function \mathcal{C} .

To test our methods, we use the same grid world setup as Scobee and Sastry (2020). Within our grid world example, shown in Figure 1, we have an action penalty of -4 for the cardinal directions, $-4 \times \sqrt{2}$ for taking the diagonal actions, and reaching the goal state has a reward of 10. In Figure 1 we set the constraint costs to various values but in all our experiments we fix the constraint costs on the generated grids for states, actions, and features to be -50 . Throughout we assume a non-deterministic world with a 10% chance of action failure, resulting in a random action.

2.3 Multi-Alternative Decision Field Theory

Multi-alternative Decision Field Theory (MDFT) is a dynamic cognitive approach that models human decision making based on psychological principles (Busemeyer and Diederich 2002; Roe, Busemeyer, and Townsend 2001). MDFT models preferential choice as an iterative cumulative process in which at each time instant the decision maker attends to a specific attribute to derive comparisons among options and update their preferences accordingly. Ultimately the accumulation of those preferences informs the decision maker’s choice. In MDFT an agent is confronted with multiple options and equipped with an initial personal evaluation for them along different criteria, called attributes. For example, a student who needs to choose a main course among those offered by the cafeteria will have in mind an initial evaluation of the options in terms of how tasty and healthy they look. More formally, an MDFT model is composed of the following (Roe, Busemeyer, and Townsend 2001):

Personal Evaluation: Given set of options $O = \{o_1, \dots, o_k\}$ and set of attributes $A = \{A_1, \dots, A_J\}$, the subjective value of option o_i on attribute A_j is denoted by m_{ij} and stored in matrix \mathbf{M} . In our example, let us assume that the cafeteria options are *Salad* (S), *Burrito* (B) and *Vegetable pasta* (V). Matrix \mathbf{M} , containing the student’s preferences, could be defined as shown in Figure 2 (left), where rows correspond to the options (S, B, V) and the columns to the attributes *Taste* and *Health*.

$$\mathbf{M} = \begin{bmatrix} 1 & 5 \\ 5 & 1 \\ 2 & 3 \end{bmatrix} \quad \mathbf{C} = \begin{bmatrix} 1 & -1/2 & -1/2 \\ -1/2 & 1 & -1/2 \\ -1/2 & -1/2 & 1 \end{bmatrix} \quad \mathbf{S} = \begin{bmatrix} +0.9000 & 0.0000 & -0.0405 \\ 0.0000 & +0.9000 & -0.0047 \\ -0.0405 & -0.0047 & +0.9000 \end{bmatrix}$$

Figure 2: Evaluation (\mathbf{M}), Contrast (\mathbf{C}), and Feedback (\mathbf{S}) matrix.

Attention Weights: Attention weights are used to express the attention allocated to each attribute at a particular time t during the deliberation. We denote them by vector $\mathbf{W}(t)$ where $W_j(t)$ represents the attention to attribute j at time t . We adopt the common simplifying assumption that, at each point in time, the decision maker attends to only one attribute (Roe, Busemeyer, and Townsend 2001). Thus, $W_j(t) \in \{0, 1\}$ and $\sum_j W_j(t) = 1, \forall t, j$. In our example, we have two attributes, so at any point in time t we will have $\mathbf{W}(t) = [1, 0]$, or $\mathbf{W}(t) = [0, 1]$, representing that the student is attending to, respectively, *Taste* or *Health*. The attention weights change across time according to a stationary stochastic process with probability distribution \mathbf{w} , where w_j is the probability of attending to attribute A_j . In our example, defining $w_1 = 0.55$ and $w_2 = 0.45$ would mean that at each point in time, the student will be attending *Taste* with probability 0.55 and *Health* with probability 0.45. In other words, *Taste* matters slightly more than *Health*.

Contrast Matrix: Contrast matrix \mathbf{C} is used to compute the advantage (or disadvantage) of an option with respect to the other options. In the MDFT literature (Busemeyer and Townsend 1993; Roe, Busemeyer, and Townsend 2001; Hotaling, Busemeyer, and Li 2010), \mathbf{C} is defined by contrasting the initial evaluation of one alternative against the average of the evaluations of the others, as shown for the case with three options in Figure 2 (center).

At any moment in time, each alternative in the choice set is associated with a **valence** value. The valence for option o_i at time t , denoted $v_i(t)$, represents its momentary advantage (or disadvantage) when compared with other options on some attribute under consideration. The valence vector for k options o_1, \dots, o_k at time t , denoted by column vector $\mathbf{V}(t) = [v_1(t), \dots, v_k(t)]^T$, is formed by $\mathbf{V}(t) = \mathbf{C} \times \mathbf{M} \times \mathbf{W}(t)$. In our example, the valence vector at any time point in which $\mathbf{W}(t) = [1, 0]$, is $\mathbf{V}(t) = [1 - 7/2, 5 - 3/2, 2 - 6/2]^T$.

In MDFT, preferences for each option are accumulated across the iterations of the deliberation process until a decision is made. This is done by using **Feedback Matrix S**, which defines how the accumulated preferences affect the preferences computed at the next iteration. This interaction depends on how similar the options are in terms of their initial evaluation expressed in \mathbf{M} . Intuitively, the new preference of an option is affected positively and strongly by the preference it had accumulated so far, while it is inhibited by the preference of similar options. This lateral inhibition decreases as the dissimilarity between options increases. Figure 2 (right) shows \mathbf{S} for our example following the MDFT method in (Hotelling, Busemeyer, and Li 2010).

At any moment in time, the preference of each alternative is calculated by $\mathbf{P}(t+1) = \mathbf{S} \times \mathbf{P}(t) + \mathbf{V}(t+1)$ where $\mathbf{S} \times \mathbf{P}(t)$ is the contribution of the past preferences and $\mathbf{V}(t+1)$ is the valence computed at that iteration. Starting with $\mathbf{P}(0) = 0$, preferences are then accumulated for either a fixed number of iterations (and the option with the highest preference is selected) or until the preference of an option reaches a given threshold. In the first case, MDFT models decision making with a *specified* deliberation time, while, in the latter, it models cases where deliberation time is *unspecified* and choice is dictated by the accumulated preference magnitude. In general, different runs of the same MDFT model may return different choices due to the attention weights' distribution. In this way MDFT induces choice distributions over set of options and is capable of capturing well know behavioral effects such as the compromise, similarity, and attraction effects that have been observed in humans and that violate rationality principles (Busemeyer and Townsend 1993).

3 Learning Soft Constraints From Demonstrations

We now describe our method for learning a set soft constraints from a set of demonstrations \mathcal{D} and a nominal MDP \mathcal{M}^N . This is the first step in our goal of providing a flexible and expressive method for orchestrating trade-offs. The method described here generalizes the work of both Scobee and Sastry (2020) and Malik et al. (2021) to the setting of non-deterministic MDPs and soft constraints.

3.1 MESC-IRL: Max Entropy Inverse Soft-Constraint Reinforcement Learning

Following Ziebart et al. (2008), our goal is to optimize a function that linearly maps the features of each transition to the reward associated with that transition, $R(s_t, a_t, s_{t+1}) = \omega \phi(s_t, a_t, s_{t+1})$, where ω is the reward weight vector. Ziebart et al. (2008) propose a maximum entropy model for

finding a unique solution (ω) for this problem. Based on this model, the probability of finite-length trajectory τ being executed by an agent traversing an MDP \mathcal{M} is exponentially proportional to the reward earned by that trajectory and can be approximated by:

$$P(\tau|\omega) \approx \frac{e^{\omega^T \phi(\tau)}}{Z(\omega)} \prod_{(s_t, a_t, s_{t+1}) \in \tau} P(s_{t+1}|s_t, a_t).$$

The optimal solution is obtained by finding the maximum likelihood of the demonstrations \mathcal{D} using this probability distribution: $\omega^* = \underset{\omega}{\operatorname{argmax}} \sum_{\tau \in \mathcal{D}} \log P(\tau|\omega)$.

We extend the problem defined in Scobee and Sastry (2020) to that of learning a set of *soft* constraints which best explain a set of observed demonstrations. This allows us to move from the notion of a constraint forbidding an action or a state to that of a soft constraint imposing a penalty proportional to the gravity of its violation. In other words, given access to \mathcal{M}^N and a set of demonstrations \mathcal{D} in ground-truth constrained MDP \mathcal{M}^{C^*} we want to find the costs \mathcal{C} . More formally, we define the residual reward function $R^R : \mathcal{S} \times \mathcal{A} \times \mathcal{S} \rightarrow \mathbb{R}_+$ as a mapping from the transitions to the penalties. We can now formally define our soft-constrained MDP \mathcal{M}^C as follows:

Definition 1 Given $\mathcal{M}^N = \langle \mathcal{S}, \mathcal{A}, P, \mu, \phi, R^N \rangle$ we define soft-constrained MDP $\mathcal{M}^C = \langle \mathcal{S}, \mathcal{A}, P, \mu, \phi, R^C \rangle$ where $R^C = R^N - R^R$.

Thus, the goal of our task is to find a residual reward function R^R that maximizes the likelihood of the demonstrations \mathcal{D} given the nominal MDP \mathcal{M}^N .

Our solution is based on adapting Maximum Causal Entropy Inverse Reinforcement learning (Ziebart et al. 2008; Ziebart, Bagnell, and Dey 2010) to soft-constrained MDPs. Following the setting of Ziebart et al. (2008) we can write the reward function R^N (resp. R^C) of \mathcal{M}^N (resp. \mathcal{M}^C) as a linear combination of the transitions: $R^N(s_t, a_t, s_{t+1}) = \omega^N \phi(s_t, a_t, s_{t+1})$ and $R^C(s_t, a_t, s_{t+1}) = \omega^C \phi(s_t, a_t, s_{t+1})$. As, both reward functions R^N and R^C are linear, R^R should be linear as well $R^R = \omega^R \phi(s_t, a_t, s_{t+1})$. From this formulation of R^R we can infer that the reward vectors follow $\omega^C = \omega^N - \omega^R$.

At this point we can use Max Entropy IRL for learning a reward function compatible with the trajectories in \mathcal{D} . The gradient for maximizing the likelihood in this setting is defined as in Ziebart et al. (2008):

$$\nabla_{\omega^C} \mathcal{L}(\mathcal{D}) = \mathbb{E}_{\mathcal{D}}[\phi(\tau)] - \sum_{(s_t, a_t, s_{t+1})} D_{s_t, a_t, s_{t+1}} \phi(s_t, a_t, s_{t+1}) \quad (1)$$

Where $D_{s_t, a_t, s_{t+1}}$ is the expected feature frequencies for transition (s_t, a_t, s_{t+1}) using the current ω^C weights. Given that the reward vectors follow $\omega^C = \omega^N - \omega^R$, we can write $\nabla_{\omega^C} = -\nabla_{\omega^R}$. Finally, by substituting this in Eq. 1 we obtain the gradient of likelihood of the constrained trajectories with respect to ω^R :

$$\nabla_{\omega^R} \mathcal{L}(\mathcal{D}) = \sum_{(s_t, a_t, s_{t+1})} D_{s_t, a_t, s_{t+1}} \phi(s_t, a_t, s_{t+1}) - \mathbb{E}_{\mathcal{D}}[\phi(\tau)] \quad (2)$$

As we estimate the residual rewards with respect to the nominal rewards, these rewards are automatically scaled to be compatible with the nominal rewards.

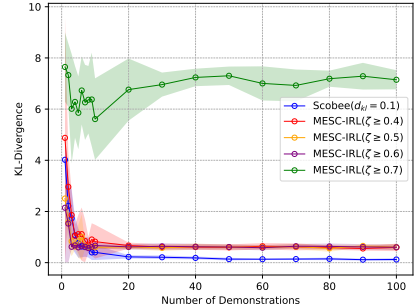
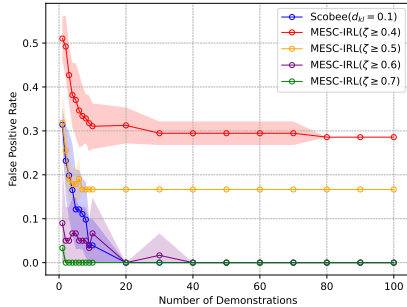


Figure 3: Comparison of MESC-IRL to the best performing method of Scobee and Sastry (2020) at recovering hard constraints in a deterministic setting according to false positive rate (left) and KL-Divergence from the demonstrations \mathcal{D} (right) as we vary the number of demonstrations. Each point is the mean of 10 independent draws.

3.2 Generalizing From Penalties to Probabilities

The estimated penalties from the previous section can effectively guide an agent to navigate the environment optimally as well as provide estimates of the cost of the constraints scaled to the value of the original reward signal. However, there may be instances, such as when comparing with hard constraints, where we desire *probabilities* that a particular action is constrained. Having probabilities allows us to compare constraints across environments with possibly different scales, allows us to use this information to guide our policies, and allows us to evaluate the confidence we have in a particular constraint. In this section we describe a method to transition from penalties to probabilities, as well as a generalized method to extract these probabilities based on a subset of the features of the environment, which can facilitate transfer learning between domains.

Intuitively, a transition where the residual reward, i.e., the penalty, is significantly larger than zero is more likely to be a constraint. We estimate the significance of a penalty by scaling it to the standard deviation of the mean learned reward. Therefore, we assume that a transition penalty is a random variable, denoted by $\mathcal{C} \sim \text{logistic}(\sigma_{pooled}, \sigma_{pooled})$, following a logistic distribution with standard deviation σ_{pooled} , where $\sigma_{pooled} = \sqrt{(\sigma_{\mathcal{N}}^2 + \sigma_{\mathcal{C}}^2)}/2$ and $\sigma_{\mathcal{N}}$ and $\sigma_{\mathcal{C}}$ are the standard deviations of the rewards in the nominal and learned constrained worlds, respectively. Informally, when penalties are close to zero, we want their probabilities to be small. To do this we set the mean of the distribution to be $\mu = \sigma_{pooled}$.

We now want to reason about a random variable ζ that indicates our belief that the transition (s_t, a_t, s_{t+1}) is forbidden. Hence using the above probability distribution we can define the probability of constraint given a transition as:

$$\zeta \equiv P(\mathcal{C} \leq R^R(s_t, a_t, s_{t+1})) = \text{sigmoid}\left(\frac{R^R(s_t, a_t, s_{t+1}) - \sigma_{pooled}}{\sigma_{pooled}}\right)$$

In our formulation, the residual rewards only depend on the features associated with them. Hence, we can use this fact to reason about constraints over only a subset of features \mathbf{f} , e.g., only color or state position. Let $\phi_f \subseteq \phi$ be the subset of features we are concerned with. In our grids we represent ϕ with a vector of length 92. The first 81 elements represent the states, the next 8 represent the actions, and the last 3

represent the colors. So if we are interested in only learning about constraints over the colors, ϕ_f will be a vector equal to the last three elements of ϕ that is $\phi_{color} \equiv \phi_{90,91,92}$.

Let ϕ_f and ω_f^R be the feature function and residual feature weight vector for \mathbf{f} . We can now define the probability of a feature value to be constrained as:

$$\zeta_f \equiv P(\mathcal{C} \leq \omega_f^R \phi_f) = \text{sigmoid}\left(\frac{\omega_f \phi_f - \text{std}_{pooled}}{\text{std}_{pooled}}\right).$$

3.3 Experimental Evaluation of MESC-IRL

In this section we empirically validate our method for soft constraint learning against both the method of Scobee and Sastry (2020) for learning hard constraints in deterministic settings as well as on learning soft constraints in non-deterministic settings. Figure 3 shows the performance of MESC-IRL compared to the method proposed by Scobee and Sastry (2020) on the same metrics from their paper: false positives, i.e., predicting a constraint when one does not exist, and KL-Divergence from the demonstrations set \mathcal{D} . For this test we use the same single grid, hard constraints, and a deterministic setting to allow for a direct comparison. We generate 10 independent sets of 100 demonstrations and report the mean. In order to decide if the values returned by MESC-IRL represent a hard constraint, we threshold the value of ζ at various levels and plot the comparison to the best result from Scobee and Sastry (2020). MESC-IRL with $\zeta \geq 0.6$ performs better than existing methods when the number of demonstrations is low, about the same when there are more demonstrations, and is able to also work for soft constraints and non-deterministic settings.

In order to evaluate MESC-IRL on soft constraints we need to adapt the notion of false positives and false negatives. Let a false positive fp be:

$$fp = \frac{|\{x \in \mathcal{C} | \mathcal{C}(x) = 0 \wedge (\zeta_{\mathcal{C}}(x) - \zeta_{\mathcal{C}^*}(x) > \chi)\}|}{\text{Num. Constraints}}$$

Where $\zeta_{\mathcal{C}}(x)$ and $\zeta_{\mathcal{C}^*}(x)$ are the predicted and true probability of transition x being constrained as described in Section 3.2, and χ is a value in $[0,1]$. Intuitively, we count a constraint as a false positive whenever there is no constraint in $\mathcal{M}^{\mathcal{C}^*}$ and the predicted probability exceeds the true proba-

bility by more than the threshold χ . We can adapt the notion of false negatives, fn in the same way by taking $c(x) \neq 0$.

Figure 4 shows the results of our tests on recovering soft constraints in non-deterministic settings with random grids, results for deterministic settings can be found in the Appendix. For these tests we choose a start and a goal state randomly at least 8 moves apart, set 6 states for blue, 6 for green randomly, and select 6 randomly constrained states; all penalties are set to -50 . Again we take 10 sets of 100 demonstrations. We see a strong decrease in both false positives and false negatives as the number of demonstrations grows. We see that in general, and even more so when the optimal threshold $\chi = 0.2$ is selected, our method almost never adds constraints that are not present in the ground truth and rarely underestimates the probability of existing ones, even for relatively small demonstration sets. Likewise our method is able to generate trajectories very close to \mathcal{D} , showing that we are able to recover both constraints and behavior even with soft constraints in non-deterministic setting. Hence MESC-IRL is able to work across a variety of settings and accurately capture demonstrated constraints.

4 Orchestrating Goals and Constraints

Often humans are confronted with decisions that require making trade-offs between collective norms and personal objectives (Rossi and Mattei 2019; Noothigattu et al. 2019). In this section we investigate different ways to model this orchestration in constrained grid environments. We consider different methods for combining policies π_n for the nominal \mathcal{M}^N and π_c for the learned constrained \mathcal{M}^C . For every state action pair (s, a) we consider vectors $\langle sq_n(s, a_i) \rangle$ and $\langle sq_c(s, a_i) \rangle$ with $i \in \{1, \dots, k\}$ where $sq_n(s, a_i)$ (resp. $sq_c(s, a_i)$) represents the probability of choosing action a_i in state s according to policy π_n (resp. π_c). They are obtained by taking the softmax of the Q-values for each policy:

Greedy (π_G): Let $\pi_G(s) = a$, where each a is the one with highest Q-value, $a = \underset{a \in \mathcal{A}_s}{\operatorname{argmax}} \max\{q_c(s, a), q_n(s, a)\}$.

Weighted Average (π_{WA}): Given weight vector (w_n, w_c) with $w_n, w_c \in [0, 1]$ and $w_c + w_n = 1$, action $a = \pi_{WA}(s)$ is chosen according to probability distribution $p_{WA}(a_i) = w_n sq_n(s, a_i) + w_c sq_c(s, a_i)$.

MDFT (π_{MDFT}): Action $a = \pi_{MDFT}(s)$ is chosen via an MDFT model where: \mathbf{M} is a $k \times 2$ matrix where rows (i.e., options) correspond to actions and columns (i.e., attributes) correspond to \mathcal{M}^N and \mathcal{M}^C . The i -th element of the respective world column is $sq_n(s, a_i)$ (resp., $sq_c(s, a_i)$), i.e., we are using the probability of choosing an action as a proxy of its preference. The weight vector (w_n, w_c) is defined as for π_{WA} , and serves as probability distribution \mathbf{w} defining how attention shifts between attributes during deliberation. Matrices \mathbf{C} and \mathbf{S} are defined in the standard way as described in Section 2.3. When reaching state s , an MDFT deliberation process is launched to decide which action should be chosen. At each step the focus is shifted to \mathcal{M}^N or \mathcal{M}^C according to probability distribution (w_n, w_c) , and the preferences

of the actions according to the selected attribute are accumulated as per Section 2.3.

Informally, Greedy is a deterministic approach that takes the most promising action, WA allows the agent to prioritize the pursuit of the goal state and satisfying constraints via a new policy obtained by considering the weighted average of the nominal and constrained distributions, and the MDFT-based orchestrator uses MDFT to chose at each step an action as suggested by the MDFT machinery.

4.1 Comparison of Orchestration Methods

We first compare theoretically the expressive power of the three orchestrators. We focus on a single state s and consider how the policies compare in terms of being able to model a given distribution over the actions available in s . We start by considering the Greedy orchestrator that is deterministic and will pick a fixed action a in state s . Both WA and MDFT can model the Greedy policy by shifting all the weight to the environment where the maximum value is obtained and zeroing all preferences except for that of action a . A formal description is provided in the Appendix. This observation, along with the fact that MDFT and WA are non-deterministic, allows us to conclude that Greedy is strictly less expressive than the other two orchestrators.

Turning to the comparison between MDFT and WA, we can prove the following statement.

Theorem 1 *Given any state s , there exist choice probability distributions over the actions available in s that can be modeled by MDFT but not by WA.*

We use an instance of the well known compromise effect (Busemeyer and Diederich 2002) according to which a compromising alternative tends to be chosen more often by humans than options with complementary preferences with respect to the attributes. Consider the case of state s with three actions a_1, a_2 and a_3 . Let us assume that, for example, $sq_n(s, a_1) = 1/6, sq_n(s, a_2) = 1/3, sq_n(s, a_3) = 1/2$ and $sq_c(s, a_1) = 1/2, sq_c(s, a_2) = 1/3, sq_c(s, a_3) = 1/6$. According to the compromise effect humans will tend to choose a_2 more often than a_1 and a_3 . Such a choice distribution over the actions can be modeled by an MDFT defined over option set $\{a_1, a_2, a_3\}$, with two attributes and weights $w_n = 0.55$ and $w_c = 0.45$ (Busemeyer and Diederich 2002). However, if we now consider WA, we can see that there is no way to define weights (w_n, w_c) such that the corresponding weighted average probability satisfies $w_n sq_n(s, a_2) + w_c sq_c(s, a_2) > \max\{w_n sq_n(s, a_1) + w_c sq_c(s, a_1), w_n sq_n(s, a_3) + w_c sq_c(s, a_3)\}$. Thus, this distribution over actions cannot be modeled by the WA.

On the other hand, if we consider MDFTs in general, i.e. without the restriction of having two attributes, we can model any distribution. Intuitively this is achieved by defining an MDFT model over k actions and with k attributes where the weight of the i -th attribute corresponds to the probability of the i -th action. Matrix \mathbf{M} is set to the identity matrix and deliberation is halted after one iteration; see the Appendix for details.

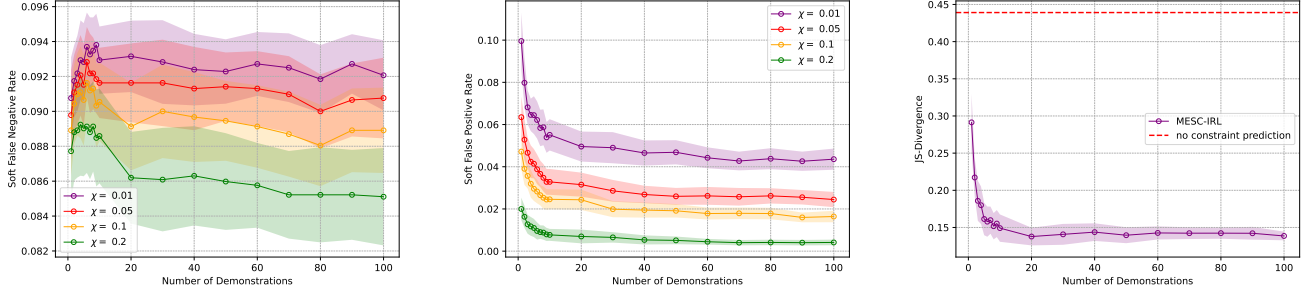


Figure 4: Performance of MESC-IRL on recovering soft constraints in non-deterministic settings according to false negatives (left), false positives (center), and JS-Divergence to \mathcal{D} (right). We see that across all these settings we are able to accurately recover constraints and generate behavior similar to the \mathcal{D} even with few demonstrations.

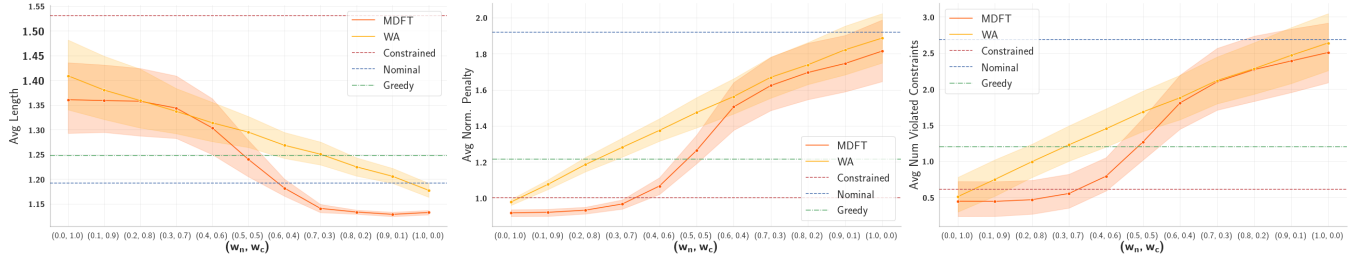


Figure 5: Comparison of the three orchestrators (Greedy, WA, and MDFT) on metrics including average path length (left), normalized penalty (lower is better, center), and average number of violated constraints (lower is better, right). We see that across all the metrics the MDFT orchestration is able to generate shorter paths that incur less penalty and violate fewer constraints.

Theorem 2 Given a s and the set A_s of actions available in s , consider a probability distribution p defined over A_s . We can define an MDFT model where the set of options corresponds to A_s and the induced choice probability distribution coincides with p .

As a consequence, MDFT is general enough to express the probability distributions induced over the actions by WA. Whether this is true also in the case of MDFT with only two attributes, as used in π_{MDFT} , remains an open theoretical question. However, we can see this experimentally: in Rahgooy and Venable (2019) the authors propose an RNN-based approach that starts from samples of a choice distribution and recovers parameters of an MDFT model, minimizing the divergence between the original and MDFT-induced choice distributions. We adapt their code¹ and generate 100 instances of WA distributions starting from random sq_n and sq_c distributions and (w_n, w_c) weights. For each of these instances we generate 100 samples (i.e. chosen actions). We fix the sq_n and sq_c values as parameters for the M matrix and learn the attention weight distribution w using 300 learning iterations. We use the learned MDFT model to generate a choice distribution over the actions with a stopping criteria of 25 deliberations steps. The observed average JS divergence between the original WA distributions and the ones induced by learned MDFT is 0.024 with standard error

¹Available at <https://github.com/Rahgooy/MDFT>

0.0013; showing experimentally we can learn weights for an MDFT model to replicate any choice distribution of WA.

4.2 Experimentally Evaluating Orchestrators

We compare the orchestrators empirically with the goal of testing if the combination of MESC-IRL with the orchestration techniques can be leveraged to create agents that trade-off between conflicting objectives like humans.

We start by generating 100 different non-deterministic nominal worlds, \mathcal{M}^N , as described in Sections 2 and 3. We learn, via VI on \mathcal{M}^{C^*} the optimal policy in the (ground truth) constrained world, denoted π_{C^*} and, similarly to Scobee and Sastry (2020), we use it to generate sets of 200 demonstrations, \mathcal{D} . We then pass \mathcal{D} to MESC-IRL, and the learned constraints are added to \mathcal{M}^N yielding the learned constrained MPD, \mathcal{M}^C . We use VI on \mathcal{M}^N and \mathcal{M}^C to obtain π_n and π_c , and we consider different ways to prioritize them by sweeping the weight values (w_n, w_c) from $(0, 1)$ to $(1, 0)$ in steps of 0.1. Note that at $(1, 0)$ (resp. $(0, 1)$) WA is equivalent to π_n (resp. π_c), and that in both cases MDFT becomes deterministic, picking the action with highest Q-value.

For all our results we generated 200 trajectories for each step and method (including π_n and π_c , denoted as Nominal and Constrained in Fig. 5), and for each of the 100 random worlds. We first perform the Kolmogorov-Smirnov test to see if the trajectories generated by WA and MDFT induce the same distribution (H_0). We reject H_0 at every weight

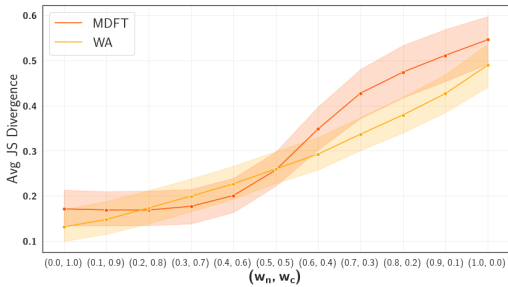


Figure 6: Average JS Divergence between policies generated with π_c and orchestrators MDFT and WA.

step with $p_value \leq 0.01$, thus the two techniques induce statistically significantly different choice distributions.

Figure 5 (left) shows the average length of trajectories produced by the orchestrators normalized so that 1.0 is the shortest path between the start and goal state; (center) we scale the penalty by the average penalty for trajectories in \mathcal{M}^C , lower is better; (right) we show the average number of violated constraints. Across all these metrics, the MDFT agent is performing better than WA by always reaching the goal in a smaller number of steps no matter the configuration of the orchestrator. We can also see that the MDFT agent violates fewer constraints and accumulates lower penalties.

Finally, in Figure 6 we show the JS Divergence between the trajectories generated by π_{C^*} and the trajectories generated by MDFT and WA, as the weight vector varies. For both agents, the divergence is small on the left and grows moving to the right, as constraints become less important. This is not surprising, since the reference trajectories are generated using π_{C^*} . Furthermore, we note that the MDFT advantage is more significant when w_c is larger, that is when constraints matter more. An explanation for this is that a large value w_c results in more MDFT deliberation steps to be focused (exclusively) on preferences relative to the constrained world. In WA, the averaging of the values underlying the policies, although weighted, is not able to maintain the importance of the constraints.

5 Conclusions and Future Work

We proposed a novel and general constraint learning method combined with a unique agent architecture aimed at learning constraints from demonstrations and exhibiting human-like trade-offs in environments with competing objectives. Our theoretical and experimental results show that the MDFT-based method exhibits superior expressive power and performance both in terms of the quality of the produced trajectories as well as capability of capturing initial demonstrations. Another important features of this cognitive approach is its effectiveness in capturing behavioral traits of humans decision making, a key factor for real life applications involving human-generated demonstrations and decisions. Our MESC-IRL approach is a general approach for learning soft constraints over actions, states, and features in non-deterministic decision making environments.

We plan to run experiments with human decision makers

and employ also learning-based orchestrators Noothigattu et al. (2019). We are also working on a novel multi-agent architecture with several orchestrators acting as either reactive or deliberate agents, e.g., the system 1 / system 2 model of Kahneman (2011) with a meta-cognitive agent to arbitrate, with the goal of further advancing the performance and generality of decision making agents.

References

- Abbeel, P.; and Ng, A. Y. 2004. Apprenticeship learning via inverse reinforcement learning. In *Proceedings of the 21st International Conference on Machine Learning (ICML)*.
- Altman, E. 1999. *Constrained Markov Decision Processes*, volume 7. CRC Press.
- Amodei, D.; Olah, C.; Steinhardt, J.; Christiano, P.; Schulman, J.; and Mané, D. 2016. Concrete problems in AI safety. *arXiv preprint arXiv:1606.06565*.
- Balakrishnan, A.; Bouneffouf, D.; Mattei, N.; and Rossi, F. 2018. Using Contextual Bandits with Behavioral Constraints for Constrained Online Movie Recommendation. In *Proc. of the 27th Intl. Joint Conference on AI (IJCAI)*.
- Balakrishnan, A.; Bouneffouf, D.; Mattei, N.; and Rossi, F. 2019. Incorporating Behavioral Constraints in Online AI Systems. In *Proc. of the 33rd AAAI Conference on Artificial Intelligence (AAAI)*.
- Booch, G.; Fabiano, F.; Horesh, L.; Kate, K.; Lenchner, J.; Linck, N.; Loreggia, A.; Murugesan, K.; Mattei, N.; Rossi, F.; and Srivastava, B. 2021. Thinking Fast and Slow in AI. In *Thirty-Fifth AAAI Conference on Artificial Intelligence, AAAI 2021, Thirty-Third Conference on Innovative Applications of Artificial Intelligence, IAAI 2021, The Eleventh Symposium on Educational Advances in Artificial Intelligence, EAAI 2021, Virtual Event, February 2-9, 2021*, 15042–15046. AAAI Press.
- Bussemeyer, J. R.; and Diederich, A. 2002. Survey of decision field theory. *Mathematical Social Sciences*, 43(3): 345–370.
- Bussemeyer, J. R.; and Townsend, J. T. 1993. Decision field theory: a dynamic-cognitive approach to decision making in an uncertain environment. *Psychological review*, 100(3): 432.
- Chou, G.; Berenson, D.; and Ozay, N. 2018. Learning constraints from demonstrations. *arXiv preprint arXiv:1812.07084*.
- Hotelling, J. M.; Bussemeyer, J. R.; and Li, J. 2010. Theoretical developments in decision field theory: Comment on Tsetsos, Usher, and Chater (2010). *Psychological Review*, 117(4).
- Kahneman, D. 2011. *Thinking, Fast and Slow*. Macmillan.
- Malik, S.; Anwar, U.; Aghasi, A.; and Ahmed, A. 2021. Inverse Constrained Reinforcement Learning. In Meila, M.; and Zhang, T., eds., *Proceedings of the 38th International Conference on Machine Learning*, volume 139 of *Proceedings of Machine Learning Research*, 7390–7399. PMLR.
- Ng, A. Y.; and Russell, S. J. 2000. Algorithms for Inverse Reinforcement Learning. In *Proceedings of the Seventeenth*

- International Conference on Machine Learning, ICML '00*, 663–670. San Francisco, CA, USA: Morgan Kaufmann Publishers Inc. ISBN 1-55860-707-2.
- Noothigattu, R.; Bouneffouf, D.; Mattei, N.; Chandra, R.; Madan, P.; Varshney, K. R.; Campbell, M.; Singh, M.; and Rossi, F. 2019. Teaching AI agents ethical values using reinforcement learning and policy orchestration. *IBM J. Res. Dev.*, 63(4/5): 2:1–2:9.
- Rahgooy, T.; and Venable, K. B. 2019. Learning Preferences in a Cognitive Decision Model. In Zeng, A.; Pan, D.; Hao, T.; Zhang, D.; Shi, Y.; and Song, X., eds., *Human Brain and Artificial Intelligence*, 181–194. Singapore: Springer Singapore. ISBN 978-981-15-1398-5.
- Ray, A.; Achiam, J.; and Amodei, D. 2019. Benchmarking safe exploration in deep reinforcement learning. *arXiv preprint arXiv:1910.01708*, 7.
- Roe, R. M.; Busemeyer, J. R.; and Townsend, J. T. 2001. Multialternative decision field theory: A dynamic connectionist model of decision making. *Psychological review*, 108(2): 370.
- Rossi, F.; and Mattei, N. 2019. Building Ethically Bounded AI. In *Proc. of the 33rd AAAI Conference on Artificial Intelligence (AAAI)*.
- Rossi, F.; Van Beek, P.; and Walsh, T. 2006. *Handbook of Constraint Programming*. Elsevier.
- Russell, S.; Dewey, D.; and Tegmark, M. 2015. Research priorities for robust and beneficial artificial intelligence. *AI Magazine*, 36(4): 105–114.
- Scobee, D. R. R.; and Sastry, S. S. 2020. Maximum Likelihood Constraint Inference for Inverse Reinforcement Learning. In *8th International Conference on Learning Representations, ICLR 2020, Addis Ababa, Ethiopia, April 26-30, 2020*. OpenReview.net.
- Sutton, R. S.; and Barto, A. G. 2018. *Reinforcement Learning: An Introduction, 2nd Edition*. Cambridge, MA, USA: A Bradford Book.
- Svegliato, J.; Nashed, S. B.; and Zilberstein, S. 2021. Ethically compliant sequential decision making. In *Proceedings of the 35th AAAI International Conference on Artificial Intelligence (AAAI)*.
- Vazquez-Chanlatte, M.; Jha, S.; Tiwari, A.; Ho, M. K.; and Seshia, S. A. 2018. Learning Task Specifications from Demonstrations. In Bengio, S.; Wallach, H. M.; Larochelle, H.; Grauman, K.; Cesa-Bianchi, N.; and Garnett, R., eds., *Advances in Neural Information Processing Systems 31: Annual Conference on Neural Information Processing Systems 2018, NeurIPS 2018, December 3-8, 2018, Montréal, Canada*, 5372–5382.
- Ziebart, B. D.; Bagnell, J. A.; and Dey, A. K. 2010. Modeling Interaction via the Principle of Maximum Causal Entropy. In Fürnkranz, J.; and Joachims, T., eds., *Proceedings of the 27th International Conference on Machine Learning (ICML-10), June 21-24, 2010, Haifa, Israel*, 1255–1262. Omnipress.
- Ziebart, B. D.; Maas, A. L.; Bagnell, J. A.; and Dey, A. K. 2008. Maximum Entropy Inverse Reinforcement Learning. In Fox, D.; and Gomes, C. P., eds., *Proceedings of the*
- Twenty-Third AAAI Conference on Artificial Intelligence, AAAI 2008, Chicago, Illinois, USA, July 13-17, 2008*, 1433–1438. AAAI Press.

Additional Material for Making Human-Like Trade-offs in Constrained Environments by Learning from Demonstrations

A Additional Graphs For Learning Constraints

Additional graphs and results for comparison with the methods of Scobee and Sastry (2020) and MESC-IRL. Figure 7 shows the stepping results for MESC-IRL.

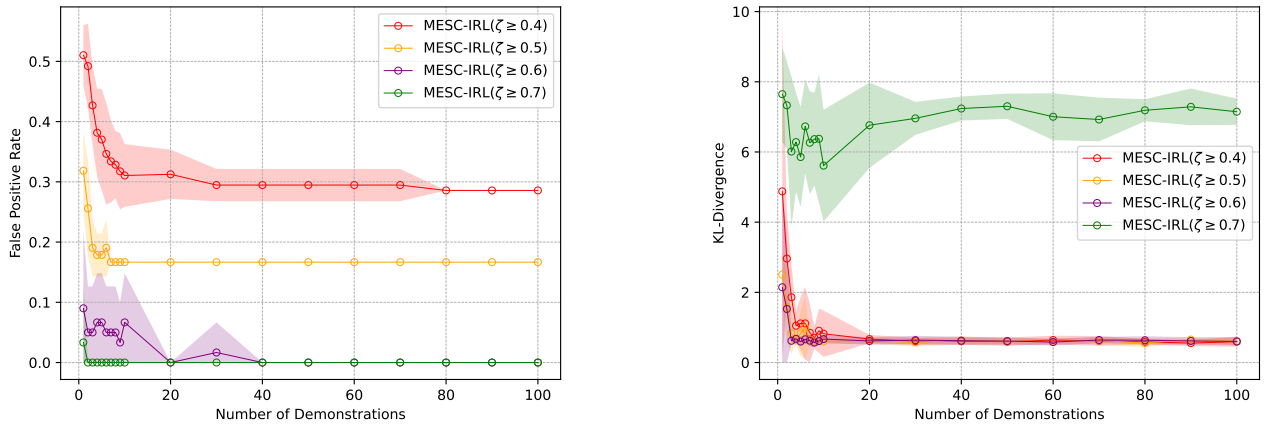


Figure 7: Performance of MESC-IRL for various settings of ζ at recovering hard constraints in a deterministic setting according to false positive rate (left) and KL-Divergence from the demonstrations \mathcal{D} (right) as we vary the number of demonstrations. Each point is the mean of 10 independent draws.

Figure 8 shows the performance of our best cutoff with the best method from Scobee and Sastry (2020).

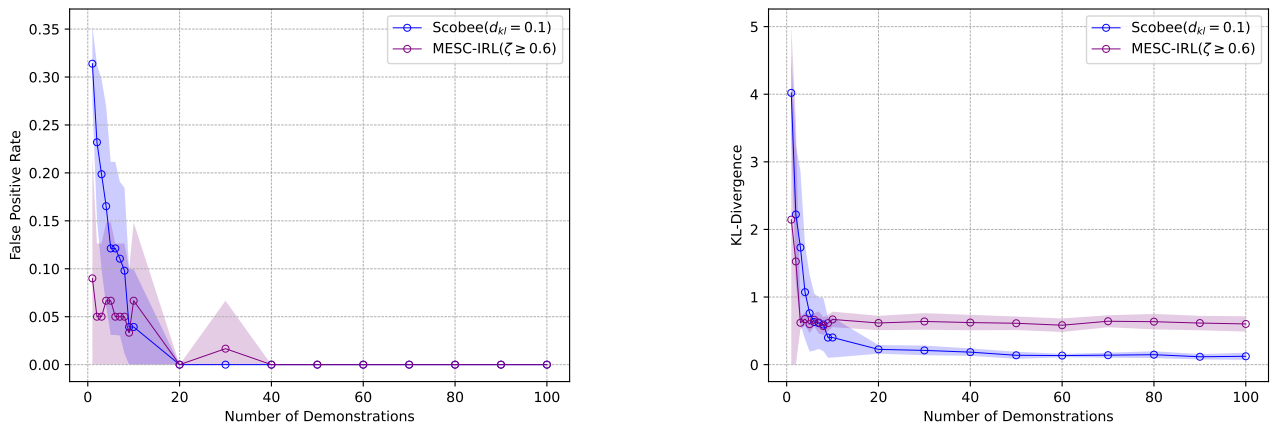


Figure 8: Comparison of the best performing version of MESC-IRL to the best performing method of Scobee and Sastry (2020) at recovering hard constraints in a deterministic setting according to false positive rate (left) and KL-Divergence from the demonstrations \mathcal{D} (right) as we vary the number of demonstrations. Each point is the mean of 10 independent draws.

Figure 9 shows the performance of MESC-IRL on recovering soft constraints in the deterministic setting.

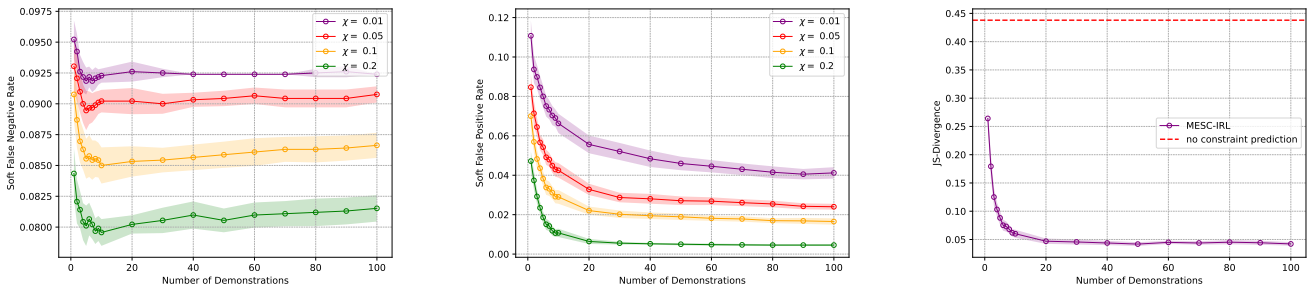


Figure 9: Performance of MESC-IRL on recovering soft constraints in deterministic settings according to false negatives (left), false positives (center), and JS-Divergence to \mathcal{D} (right). We see that across all these settings we are able to accurately recover constraints and generate behavior similar to the \mathcal{D} even with few demonstrations.

Figure 10 shows the performance of MESC-IRL on recovering soft constraints in the non-deterministic setting.

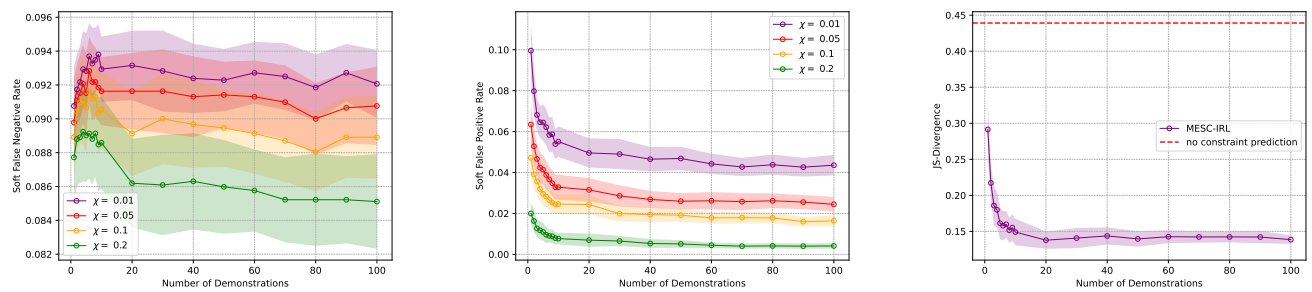


Figure 10: Performance of MESC-IRL on recovering soft constraints in deterministic settings according to false negatives (left), false positives (center), and JS-Divergence to \mathcal{D} (right). We see that across all these settings we are able to accurately recover constraints and generate behavior similar to the \mathcal{D} even with few demonstrations.

B Proof Details for Comparison of Orchestration Methods

We provide the full proofs for the theoretical comparison of the orchestrators.

Theorem 3 *Consider state s . Any choice probability distribution over the actions available in s that can be modeled by the Greedy approach can be modeled via the MDFT or WA approaches.*

Proof. We can model the (degenerate) probability distribution induced by Greedy via an MDFT with as many options as the actions available in s , two attributes with weights set to any random pair of values, and preferences in the \mathbf{M} matrix all equally to 0 except for those in the row associated with a which are set to 1. Matrices \mathbf{C} and \mathbf{S} can be defined in the standard way described in Section 2.3 and deliberation can be halted after one deliberation step. In fact, when deliberation is launched, an attribute will be selected. Regardless of which one is selected, action a will be chosen given that it is the only one with non-zero preference.

Similarly, we can model the Greedy distribution using a weighted average where $w_n = w_c = 1/2$, and $sq_n(s, a) = sq_c(s, a) = 1$ and $sq_n(s, a') = sq_c(s, a') = 0, \forall a' \neq a$. \square

Theorem 4 *Given state s and the set \mathcal{A}_s of actions available in s , consider a probability distribution p defined over \mathcal{A}_s . We can define an MDFT model where the set of options corresponds to \mathcal{A}_s and the induced choice probability distribution coincides with p .*

Prroff. Consider the MDFT model defined as follows:

- Matrix \mathbf{M} is the $k \times k$ identity matrix;
- Weight vectors \mathbf{W} are defined as in Section 2.3 and select a single attribute at each iteration. Probability distribution over attributes \mathbf{w} is defined in a way such that the probability of selecting the j -th attribute, is $p(a_j)$.
- Matrices \mathbf{C} and \mathbf{S} are defined in the standard way as described in Section 2.3.
- The deliberation time for the model is fixed at one iteration.

It is easy to see that running the model induces a choice probability over the actions which corresponds to p . In fact, in every run, which consists of a single iteration, an attribute A_h will be sampled according to probability p . Given how \mathbf{M} is defined and the fact that the initial value of the accumulated preference $\mathbf{P}(0) = 0$, action a_h will be chosen. Thus, the probability of action a_h being selected, given the MDFT model, coincides with $p(a_h)$. \square